Inorganic Chemistry

Article

pubs.acs.org/IC

Substituent Effects on the Electrochemical, Spectroscopic, and Structural Properties of Fischer Mono- and Biscarbene Complexes of Chromium(0)

Belinda van der Westhuizen,[†] Pieter J. Swarts,[‡] Louise M. van Jaarsveld,[†] David C. Liles,[†] Uwe Siegert,[‡] Jannie C. Swarts,[‡] Israel Fernández,*[,§] and Daniela I. Bezuidenhout*[,†]

[†]Chemistry Department, University of Pretoria, Private Bag X20, Hatfield 0028, Pretoria, South Africa

[‡]Chemistry Department, University of the Free State, P.O. Box 339, Bloemfontein 9300, South Africa

[§]Departamento de Química Orgánica I, Facultad de Química, Universidad Complutense, 28040 Madrid, Spain

Supporting Information

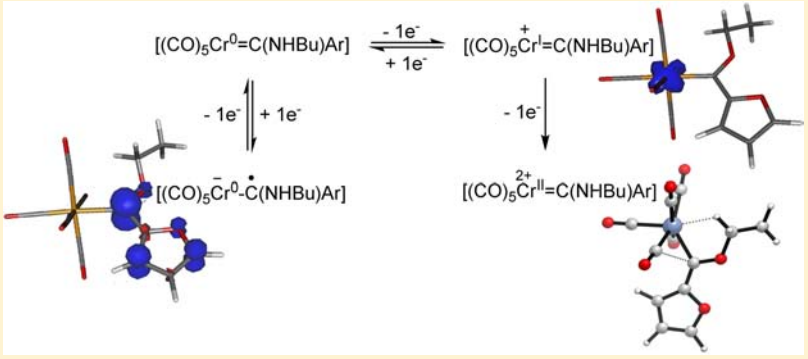

ABSTRACT: A series of ten ferrocenyl, furyl, and thienyl mono- and biscarbene chromium(0) complexes were synthesized and characterized spectroscopically and electrochemically. The single crystal structure of the biscarbene complex $[(CO)_5Cr{=}C(OEt)\text{-}Fu'\text{-}(OEt)C{=}Cr(CO)_5]$ (**4a**) was determined: $C_{20}H_{12}Cr_2O_{13}$; triclinic; $P\bar{1}$; a = 6.2838(5), b = 12.6526(9), c = 29.1888(19) Å, α = 89.575(2), β = 88.030(2), γ = 87.423(2)°; Z = 4. Results from an electrochemical study in CH_2Cl_2 were mutually consistent with a computational study in showing that the carbene double bond of **1** − **6** is reduced to an anion radical, $^{-}Cr{-}C\bullet$ at formal reduction potentials < −1.7 V vs FcH/FcH^+. The Cr centers are oxidized in two successive one electron transfer steps to Cr(II) via the Cr(I) intermediate. Only Cr(I) oxidation is electrochemically irreversible. Dicationic Cr(II) species formed upon two consecutive one-electron oxidation processes are characterized by a peculiar bonding situation as they are stabilized by genuine CH···Cr agostic interactions. With respect to aryl substituents, carbene redox processes occurred at the lowest potentials for ferrocene derivatives followed by furan complexes. Redox process in the thiophene derivatives occurred at the highest potentials. This result is mutually consistent with a ^{13}C NMR study that showed the Cr=C functionality of furyl complexes were more shielded than thienyl complexes. The NHBu carbene substituent resulted in carbene complexes showing redox processes at substantially lower redox potentials than carbenes having OEt substituents.

INTRODUCTION

The very first metal carbene complex of the type $[(OC)_5M{=}C(XR)R']$ (M = Group 6 transition metal) reported by Fischer et al. contained an aromatic phenyl substituent (R′) on the carbene carbon atom.[1] The structural data published shortly thereafter illustrated the role of the heteroatom X lone-pair in stabilizing the singlet carbene carbon, in conjunction with the metal's synergic $d(t_{2g})$-p π-interaction with the carbene carbon atom.[2] This bonding situation has been extensively studied also by means of computational tools.[3] On the other hand, the aryl substituent, R′, can be incorporated into the π-delocalized network surrounding the carbene carbon and can act as either an electron withdrawing or electron donating substituent. The general structural motif of employing heteroaromatic compounds as conjugated spacer units in mono- and biscarbene complexes has long been of interest in our laboratories.[4] In the design of complexes specifically tailored for electronic transfer processes within the molecule, and their regioselective reactions, the incorporation of the carbene ligands renders communication possible from one terminal metal to the other metal fragment via the π-frame of the molecule (Figure 1).[5]

The use of electrochemistry as a tool for the illumination of such intramolecular electronic communication wherever a convenient redox-active moiety is present is well established.[6] We have recently reported an electrochemical investigation of

Received: March 26, 2013
Published: May 17, 2013

   dx.doi.org/10.1021/ic4007422 | *Inorg. Chem.* 2013, 52, 6674−6684

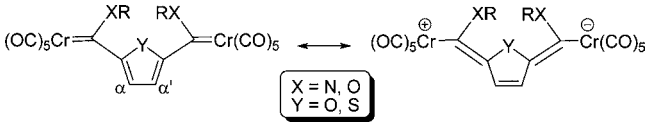

Figure 1. Stabilization of biscarbene complexes with heteroaryl spacer moieties.

thienyl mono- and biscarbene complexes of chromium(0).[7] We have shown that the Cr center of the carbene ligands undergoes electrochemical reversible one-electron oxidation to Cr(I) and thereafter it may be irreversibly oxidized in a one electron transfer process to Cr(II). The carbene formal double bond Cr=C may be reduced to $^{-}$Cr−C•. That each process represents a one electron transfer process was confirmed by comparing the intensity of each wave with the intensity of the ferrocenyl group of [(OC)$_5$Cr=C(OEt)Fc], **1**, and [(OC)$_5$Cr=C(OEt)-Fc′-(OEt)C=Cr(CO)$_5$], **2**, with linear sweep voltammetric (LSV) techniques and also by comparing i_{pc} and i_{pa} currents (c = cathodic and a = anodic, p = peak) in all cyclic voltammograms (CVs). The LSV studies were hampered by the lack of stability of the oxidized and reduced products, in that the compounds decomposed within 80 s of oxidation. On the cathodic (reducing) cycles, decomposition times were even faster. For this reason, i_{pc} and i_{pa} currents were used to interpret reversibility. Older studies of Fischer carbene complexes detail especially Cr(0) oxidation studies.[8] The revival in the interest of the electrochemical behavior of Fischer carbene complexes[9] can be attributed to the many applications of the redox activity of these complexes, including their use in organic synthesis and catalytic transformations,[10] and as electrochemical probes.[11]

The carbene substituents XR and R′ control the electrophilicity of the complex,[12] although for the heteroaryl substituents R′, stabilization of the carbene carbon atom occurs by both the conjugative release of electrons as well as specific $\pi \rightarrow$ p donation.[3d,13] Modification of the steric and electronic nature of the carbene ligand can therefore be effected by both the heteroatom and the heteroaryl substituents. To enable us to establish especially electrochemical changes that are introduced by the heteroaryl substituent we report here the synthesis, characterization, and electrochemical properties of 2-furyl (Fu) monocarbene and 2,5-furadiyl (Fu′) complexes with both the known alkoxy- and the new amino-substituted carbene carbon atoms.[14] By comparing the results with those of the 2-thienyl (Th) and 2,5-thiendiyl (Th′) biscarbene complexes of chromium(0) which we reported earlier this year,[7] we could establish a trend regarding the effects ring-heteroatom (O vs S), and carbene-heteroatom (O vs N), as well as the effect a second metal carbene moiety (mono- vs biscarbene ligands) has on the redox activity of this series of (hetero)aryl Fischer carbene complexes of chromium(0). The electrochemical results are supported by theoretical calculations which allow us to gain more insight into the nature of the species involved in the electrochemical processes. The single crystal X-ray structure of the biscarbene furan-containing complex [(CO)$_5$Cr=C(OEt)-Fu′-(OEt)C=Cr(CO)$_5$] (**4a**) is also described.

SYNTHESIS AND CHARACTERIZATION

The ethoxycarbene complexes were prepared by reaction of mono- or dilithiated (hetero)arene (ferrocene, furan, or thiophene) with 1 or 2 equiv of [Cr(CO)$_6$], followed by alkylation with 10% excess Et$_3$OBF$_4$[15] to yield the ethoxy monocarbene complexes **1**[16] and **3**,[17] or biscarbene complexes **2**[18] and **4**,[4e,f] respectively (see Scheme 1).

Aminolysis[19] of the ethoxycarbene complexes with *n*-butylamine was performed by addition of 2.2 or 4.2 mmol NH$_2$Bu to a solution of **3** (2 mmol) or **4** (2 mmol), respectively, in 20 mL of diethyl ether at room temperature. Stirring was maintained for 30 min, whereafter the solvent was removed under reduced pressure. Column chromatography with eluent hexane:CH$_2$Cl$_2$ (1:1) yielded the new furyl and thienyl aminocarbene products **5a**, **5b**[7] (monocarbene complexes), **6a** and **6b**[7] (biscarbene complexes), respectively (Scheme 1). For the monocarbene complex **5a**, NMR spectroscopy revealed the duplication of all resonances, due to the formation of both the *syn* and the *anti*-isomers (see Figure 2),[20] in a ratio of approximately 1:1. Trace amounts of isomers were observed for biscarbene complex **6a**, but only one configuration could be isolated and characterized. All neat compounds were stable in the absence of oxygen and could be stored for months at −4 °C under argon. Electrochemical

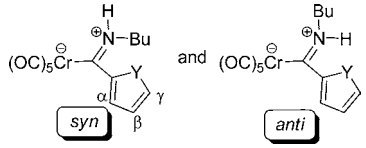

Figure 2. *Syn*- and *anti*-configuration of zwitterionic rotamers of aminocarbene complexes, with atom numbering system employed for NMR characterization.

Scheme 1. Synthesis of Chromium(0) Heteroaryl Mono- and Biscarbene Complexes

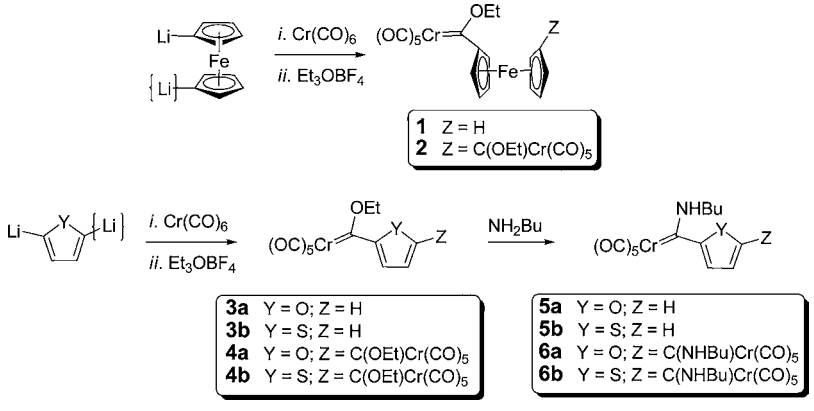

dx.doi.org/10.1021/ic4007422 | Inorg. Chem. 2013, 52, 6674−6684

evidence indicated that in CH_3CN or CH_2Cl_2 solutions, they decomposed to an observable extent within ca. 30 min at room temperature. This is slow enough to allow spectroscopic and electrochemical measurements.

Coordination of the metal-carbene moiety causes a deshielding of the α and β-protons in the ^{1}H NMR, effected by the partial positive charges afforded on these protons caused by π-resonance effects. However, unlike for the thienyl carbene complexes (**3b**−**6b**), H_α of the furyl carbene complexes (**3a**−**6a**) cannot be employed as a probe for electronic ring substituent involvement because of their upfield shift compared to H_γ (see Experimental Section). The atypical assignment of the furyl ring proton chemical shifts is based on assignments following predicted shifts for ester derivatives.[5,21] The resonances for the H_γ chemical shifts do reflect the decreased electron donation from the furyl rings for the aminocarbene complexes (**5a**, 7.67 and 7.44 ppm; **6a**, 7.13 ppm) compared to the ethoxy-analogues (**3a**, 7.82 ppm; **4a**, 7.22 ppm). The formation of both *syn*- and *anti*-rotamers across the restricted $C_{carbene}$−N bond was observed by the duplication of all NMR signals of **5a** in a ratio of 1:0.95 (*syn*:*anti*) (see Figure 2).[22] For the biscarbene complex **6a**, although three possible isomers exist (*syn,syn*; *anti,anti* or *syn,anti*), only one isomer could be observed but could not be unambiguously assigned as either the *syn,syn*- or *anti,anti*- configuration. Significant upfield shifts of the carbene carbon ^{13}C NMR resonances of the aminocarbene complexes (**5a**, 243, 250 ppm; **6a**, 250 ppm) reflect the increased $C_{carbene}$−N bond order and resultant less electrophilic carbene carbon atoms compared to **3a** (311 ppm) and **4a** (313 ppm). This corresponds to the expected decrease in the *trans*-CO stretching frequency (A_1' band)[23] of **5a** and **6a** (1910, 1916 cm^{-1}, respectively) compared to that observed for **3a** and **4a** (1960, 1962 cm^{-1}, respectively).

Comparison of ring-heteroatom effect on the ^{13}C NMR shifts of the carbene carbon atom reveals that furyl-substituted aminocarbene ligands (**5a**, **6a**) are more shielded (243, 250 ppm, respectively) than the thienyl-substituted complexes **5b** and **6b** (258−272 ppm). A smaller effect is observed when comparing thienyl ethoxycarbene ligands (**3b**, 316 ppm; **4b**, 322 ppm) with the furyl amino-analogues (**3a**, 311 ppm; **4a**, 313 ppm).

X-RAY STRUCTURAL STUDY

Complex **4a** crystallizes with two molecules in the asymmetric unit. Crystallographic data are given in Table 1. The molecular structure of molecule 1 is shown in Figure 3. The structures of both molecules are similar and are also similar to that of the methoxy-carbene analogue.[24] Selected geometric parameters (mainly about the carbene C atoms) are given in Table 2. A *trans* conformation of O_{alkoxy} and O_{furan} about the $C_{carbene}$−C_{furan} bond is electronically favored in alkoxy-furan-carbene complexes; however, in monofuran biscarbene complexes a *trans* - *trans* conformation cannot be adopted as this would bring the two $Cr(CO)_5$ moieties too close to one another and thus a *cis* - *trans* conformation is adopted.

Table 1. Crystallographic Data for 4a[a]

chemical formula: $C_{20}H_{12}Cr_2O_{13}$	formula weight: 564.30
a = 6.2838(5) Å	space group $P\bar{1}$ (No. 2)
b = 12.6526(9) Å	T = −123 °C
c = 29.1888(19) Å	λ = 0.71073 Å
α = 89.575(2)°	D_{calcd} = 1.168 g cm^{-3}.
β = 88.030(2)°	μ = 1.005 mm^{-1}
γ = 87.423(2)°	R = 0.0757 (all), 0.0478 ($I > 2\sigma I$)
V = 2316.9(3) Å^3	R_w = 0.0858 (all), 0.0786 ($I > 2\sigma I$)
Z = 4	

[a] $R = \sum||F_o| - |F_c||/\Sigma |F_o|$, $R_w = \{\sum[w(F_o^2-F_c^2)^2]/\sum[w(F_o^2)^2]\}^{1/2}$. $w = 1/[\sigma^2(F_o^2) + (0.0292P)2 + 2.2628P]$ where $P = [\mathrm{Max}(F_o^2,0) + 2F_c^2]/3$.

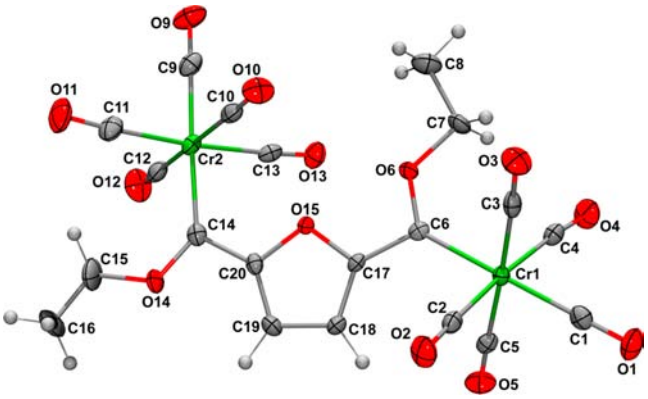

Figure 3. Ortep/PovRay[25] drawing of the structure of molecule 1 of **4a** showing the atom numbering scheme. For the atom numbering scheme of molecule 2, add 20 to each of the numbers shown. ADPs are shown at the 50% probability level.

Table 2. Selected Geometric Parameters for 4a. (Å, deg)

Cr−$C_{carbonyl}$[a]	1.889(3)	Cr−$C_{carbonyl}$[b]	1.904(9)
Cr1−C6	2.036(3)	Cr21−C26	2.049(3)
Cr2−C14	2.035(3)	Cr22−C34	2.038(3)
C6−O6	1.325(3)	C26−O26	1.317(3)
C6−C17	1.460(4)	C26−C37	1.463(4)
C14−O14	1.330(4)	C34−O34	1.326(4)
C14−C20	1.461(4)	C34−C40	1.464(4)
Cr1−C6−O6	131.0(2)	Cr21−C26−O26	131.4(2)
Cr1−C6−C17	123.7(2)	Cr21−C26−C37	123.1(2)
O6−C6−C17	105.3(2)	O26−C26−C37	105.4(2)
Cr2−C14−O14	132.5(2)	Cr22−C34−O34	132.3(2)
Cr2−C14−C20	124.0(2)	Cr22−C34−C40	123.8(2)
O14−C14−C20	103.4(3)	O34−C34−C20	103.9(2)
O6−C6−C17−O15	−5.3(3)	O26−C26−C37−O35	−3.3(3)
O14−C14−C20−O15	−174.5(2)	O34−C34−C40−O35	−174.4(3)

[a] Mean bond distance for carbonyls *trans* to a carbene. [b] Mean bond distance for carbonyls *cis* to a carbene.

ELECTROCHEMISTRY

Cyclic voltammetry (CV), linear sweep voltammetry (LSV), and Osteryoung square-wave voltammetry (SW) were conducted on 0.5 mmol dm^{-3} solutions of **1**−**6** in dry, oxygen-free CH_2Cl_2 utilizing 0.1 mol dm^{-3} $[N(n\mathrm{Bu})_4][PF_6]$ as supporting electrolyte. Data are summarized in Table 3, CVs are shown in Figures 4 and 5 while Figure 6 summarizes potential shifts due to changes in aryl, OEt or NHBu carbene substituent.

Three carbene-based redox processes were observed. These are as follows:

dx.doi.org/10.1021/ic4007422 | Inorg. Chem. 2013, 52, 6674−6684

Table 3. Cyclic Voltammetry Data of 0.5 mmol dm^{-3} solutions of the Monocarbene $[(OC)_5Cr{=}C(Ar)(X)]$ and Biscarbene Complexes $[(OC)_5Cr{=}C(X)\text{-}Ar'\text{-}(X)C{=}Cr(CO)_5]$ in CH_2Cl_2, Containing 0.1 mol dm^{-3} $[N(nBu)_4][PF_6]$ as Supporting Electrolyte at a Scan Rate of 100 mV s^{-1} and 20 °C (Potentials are Relative to the FcH/FcH$^+$ Couple)

complex	peak no.	$E^{\circ\prime}$/V, ΔE/mV	$i_{pa}/\mu A$, i_{pc}/i_{pa}
1	I(=)	−2.148, 111	3.20[b], 0.41
Ar = Fc	1($Cr^{0/I}$)	0.289, 102	3.48, 0.89
X = OEt	(Fc)	0.700, 89	3.29, 0.85
	2($Cr^{I/II}$)	*a*, *a*	*a*, *a*
2	I(=)	−1.845, 104	3.81[b], 0.39
Ar′ = Fc′	1a($Cr^{0/I}$)	0.499, 83	3.71, 0.73
X = OEt	1b($Cr^{0/I}$)	0.650, 80	3.51, 0.23
	(Fc)	0.730, 97	3.78, < 0.1
	2($Cr^{I/II}$)	*a*, *a*	*a*, *a*
3a	I(=)	−1.883, 120	3.54[b], 0.59
Ar = Fu	1($Cr^{0/I}$)	0.498, 129	3.75, 0.89
X = OEt	2($Cr^{I/II}$)	*a*, *a*	*a*, *a*
3b	I(=)	−1.762, 98	3.71[b], 0.43
Ar = Th	1($Cr^{0/I}$)	0.565, 85	3.98, 0.88
X = OEt	2($Cr^{I/II}$)	*a*, *a*	*a*, *a*
4a	D(=)[h]	−2.075, 110	3.31[b], 0.73
Ar′ = Fu′	I(=)	−1.772, 65	0.89[b], 0.73
X = OEt	1($Cr^{0/I}$)	0.565, 62	1.21, 0.74
	1($Cr^{I/II}$)	1.100[d], *d*	2.93[d], *d*
4b	D(=)[h]	−2.091, 88	1.89[b], 0.59
Ar′ = Th′	I(=)	−1.765, 232	0.68[b], 0.78
X = OEt	1($Cr^{0/I}$)	0.576, 68	0.81, 0.81
	1($Cr^{I/II}$)	1.098[d], *d*	2.50[d], *d*
5a	I(=)	−2.398[e], *e*	3.26[b], -
Ar = Fu	1a($Cr^{0/I}$)	0.340, 68	1.94, 0.91[f]
X = NHBu	1b($Cr^{0/I}$)	0.402, 98	2.86, 0.87[f]
	2($Cr^{I/II}$)	*a*, *a*	*a*, *a*
5b	I(=)	−2.232, 132	3.21[b], 0.11
Ar = Th	1a($Cr^{0/I}$)	0.258, 242	1.83, 0.80
X = NHBu	1b($Cr^{0/I}$)	0.435[c], *c*	1.75, *c*
	2($Cr^{I/II}$)	0.951[c], *c*	7.02, *c*
6a	I(=)[g]	−2.057[e], *e*	0.90[b], -
Ar′ = Fu′	1($Cr^{0/I}$)	0.430, 90	1.43, 0.77
X = NHBu	1($Cr^{I/II}$)	*a*, *a*	*a*, *a*
6b	I(=)	*a*, *a*	*a*, *a*
Ar′ = Th′	1($Cr^{0/I}$)	0.399, 138	4.81, 0.69
X = NHBu	2($Cr^{I/II}$)	1.150[d], *d*	7.42[d], *d*

[a]No peak detected within the solvent potential window. [b]i_{pc} and i_{pa}/i_{pc} values to maintain the current ratio convention of $i_{forward\ scan}/i_{reverse\ scan}$. [c]Estimated E_{pa}; poor resolution disallowed estimates of E_{pc} or i_{pa}/i_{pc}. [d]E_{pa} value, no E_{pc} detected. [e]E_{pc} value, no E_{pa} detected. [f]Estimations only. [g]Prior to peak I, a small peak was detected at −1.778 V, i_{pc} = 0.33 μA. This current is so small that it is not regarded as part of the system. [h]Peaks labeled "D" represent decomposition processes of −Cr−C• radical anions that were generated at the redox process labeled "I".

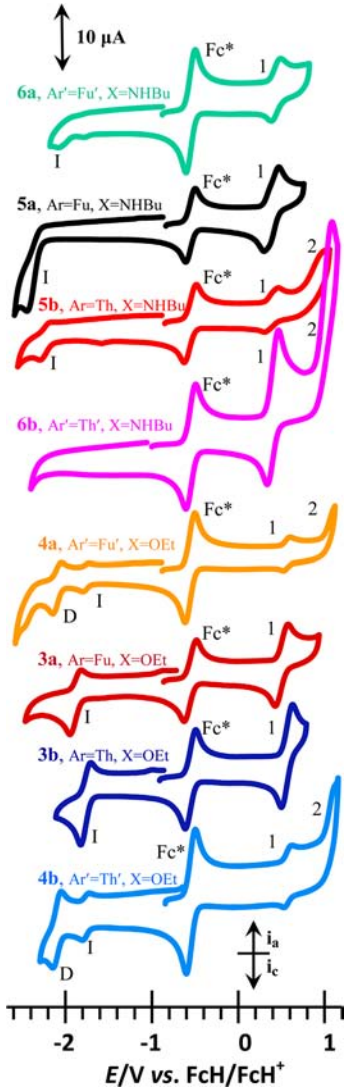

Figure 4. CVs of 0.5 mmol dm^{-3} solutions of monocarbenes **3a**, **3b**, **5a**, **5b**$[(OC)_5Cr{=}C(Ar)X]$ and biscarbenes **4a**, **4b**, **6a**, and **6b** $[(OC)_5Cr{=}C(X)\text{-}Ar'\text{-}(X)C{=}Cr(CO)_5]$ in CH_2Cl_2/0.1 mol dm^{-3} $[N(nBu)_4][PF_6]$ on a glassy carbon-working electrode at a scan rate of 400 mV/s. Decamethylferrocene, Fc*, was used as internal standard. For **4a**, **5b**, **6a**, and **6b**, concentrations were 0.25 mmol dm^{-3} for better clarity. Peaks labeled "D" represent decomposition processes of electrochemically generated $^-Cr{-}C^\bullet$ radical anions at the redox process labeled "I".

(a) The one-electron reduction of the carbene double bond; peaks for this process are labeled I throughout in Figures 4 and 5 and Table 3.

(b) Oxidation of the Cr(0) center to Cr(I) is associated with peak 1.

(c) Peaks labeled 2 are associated with the one-electron oxidation of the electrochemically generated Cr(I) center to Cr(II).

One-electron oxidation of the ferrocenyl group in **1** and **2** (peak Fc in Table 3 and Figure 4) is observed after Cr(0) oxidation but before Cr(I) and has been thoroughly described in our previous report.[7] It should be noted that it is very difficult to separate redox events that take place at closely overlapping potentials by electrochemical techniques, as discussed in detail by Taube et al.[26]

Reduction in aprotic solvents of alkenes[27] in general and the carbene double bond, Cr=C, in particular[7] are known to occur at far negative applied potentials. During a one-electron transfer process a radical anion of considerable instability is generated;

dx.doi.org/10.1021/ic4007422 | Inorg. Chem. 2013, 52, 6674−6684

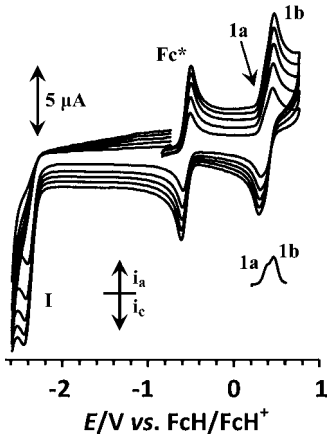

Figure 5. CVs of **5a**, (0.5 mol dm^{-3}, [(OC)$_5$Cr=C(NHBu)Fu]) in CH_2Cl_2/0.1 mol dm^{-3} [N(*n*Bu)$_4$][PF$_6$] on a glassy carbon-working electrode at scan rates of 100 (smallest currents), 200, 300, 400, and 500 mV/s. Decamethylferrocene, Fc*, was used as internal standard. The Cr$^{0/I}$ couple at peak 1 splits into two components a and b, as highlighted by the SW at 20 Hz.

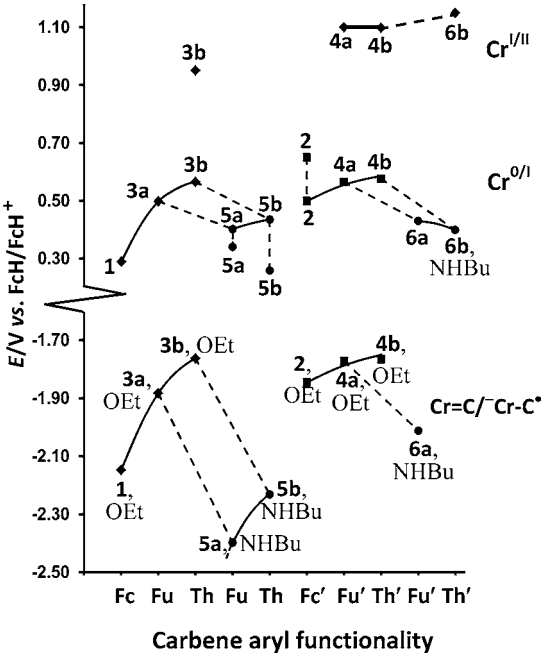

Figure 6. Redox potential changes for the Cr=C/$^-$Cr−C$^•$, Cr$^{0/I}$ and Cr$^{I/II}$ couples as a function of aryl (Ar or Ar′ = Fc or Fc′, Fu or Fu′, Th or Th′), or X = OEt or NHBu substituents in monocarbenes [(OC)$_5$Cr=C(X)Ar] **1**, **3a**, **3b**, **5a**, and **5b** as well as the biscarbenes [(OC)$_5$Cr=C(X)-Ar′-(X)C=Cr(CO)$_5$] **2**, **4a**, **4b**, **6a**, and **6b**. Cr=C reduction for **6b** fell outside the solvent potential window, as did Cr(I) oxidation to Cr(II) for **1**, **3a**, **5a**, **5b**, and **6a**. During Cr(0) oxidation of **5a**, **5b**, and **2**, two poorly resolved redox processes were observed.

follow-up chemical reactions destroy this electrochemically generated species quickly.[7]

Electrochemical reversible one-electron transfer processes are characterized by ΔE_p = 59 mV and peak current ratios approaching 1.[28] All ethoxy mono- and biscarbene complexes [(OC)$_5$Cr=C(OEt)Ar] and [(OC)$_5$Cr=C(OEt)-Ar′-(OEt)C=Cr(CO$_5$)] **1**, **2** (Ar = Fc), **3a**, **4a** (Ar = Fu), and **3b** and **4b** (Ar = Th), exhibited pseudo electrochemical reversible one-electron reduction ($\Delta E_p = E_{pa} - E_{pc} > 88$ mV, $0.39 < i_{pa}/i_{pc} < 0.73$) of the Cr=C functionality to $^-$Cr−C• at $E^{\circ\prime} < -1.762$ V vs FcH/FcH$^+$. The assignment of $^-$Cr−C• as reduction product is mutually consistent with the computational studies described below, and also with single electron transfer reactions followed by ESI-MS that indicated the formation of such species.[29] For the NHBu mono- [(OC)$_5$Cr=C(NHBu)Ar] and biscarbene [(OC)$_5$Cr=C-(NHBu)-Ar′-(NHBu)C=Cr(CO)$_5$] complexes **5a**, **6a** (Ar = Fu), **5b** and **6b** (Ar = Th), only **5b** exhibited partial chemical reversibility during Cr=C reduction (i_{pa}/i_{pc} = 0.11, Table 3, Figure 5). The other complexes exhibited electrochemical and chemical irreversible behavior for this process with i_{pa}/i_{pc} = 0. Potentials were, however, independent of scan rate between 100 and 500 mV s^{-1} (Figure 6). We conclude the reduced $^-$Cr−C• species of the NHBu derivatives are much more reactive than their OEt counter parts.

Figure 7 shows the computed frontier molecular orbitals of **3a**.[30] The highest occupied molecular orbital (HOMO) is located in a d atomic orbital of the chromium atom whereas the lowest unoccupied molecular orbital (LUMO) is mainly centered in the p_z atomic orbital of the carbene carbon atom. Therefore, it should be expected that the one-electron reduction process should lead to the radical anion **3a**$^{\bullet-}$ whose unpaired electron remains mainly located on the p_z orbital of the carbene carbon atom. Indeed, the computed spin density on **3a**$^{\bullet-}$ indicates a value of 0.60 e on the carbene carbon atom thus confirming the assignment of $^-$Cr−C• as reduction product. Similar LUMOs were observed for the rest of the mono- and biscarbene complexes.

The carbene double bond, Cr=C, of the present series of compounds benefits from the presence of the electron-donating furyl, thienyl, or ferrocenyl group which allows for conjugation (Figure 1). Conjugated substituents that have different electron donating capabilities are known to alter the redox potential of a redox active species: the more electron-donating a substituent is, the more the redox potential shifts to smaller values.[31] Nonconjugated substituents also influence the redox potentials of a redox active species but to a much lesser degree. It was found that if a substituent functionality is separated by an alkyl chain of more than four isolating (i.e., nonconjugated) carbon atoms from the redox active site, the redox active site is essentially not influenced by the substituent functionality.[32] The influence of three different conjugated aryl groups, ferrocenyl, furyl, and thienyl, as well as OEt and NHBu functionalities on the potential of Cr=C reduction is highlighted in this study.

One-electron Cr=C reduction to $^-$Cr−C• for the ethoxy monocarbenes [(OC)$_5$Cr=C(OEt)Ar] were observed at −2.148 V vs FcH/FcH$^+$ for **1** (Ar = Fc), −1.883 for **3a** (Ar = Fu), and −1.762 V for **3b** (Ar = Th; $\Delta E^{\circ\prime} = E^{\circ\prime}_{Th,3b} - E^{\circ\prime}_{Fu,3a}$ = 121 mV; Figures 4 and 6, Table 3). These observed redox potentials show how aryl groups with different electron-donating capabilities influence $E^{\circ\prime}$. The strong electron-donating capability of the ferrocenyl group is known,[33] and from the above potentials it is evident that the observed electron-donating capability of the furyl group in the chromium-ethoxy carbenes is less than that of ferrocenyl, while thienyl is the weakest electron-donating aryl group in the present series of compounds. The observed electrochemical trend nicely correlates with the computed energy of the corresponding LUMO: −2.12 eV (Ar = Fc) > −2.52 eV (Ar = Fu) > −2.69 eV (Ar = Th) which shows that a less stabilized (i.e., less negative) LUMO is translated into a higher reduction potential. In addition, this result supports the finding of the ^{13}C

dx.doi.org/10.1021/ic4007422 | Inorg. Chem. 2013, 52, 6674−6684

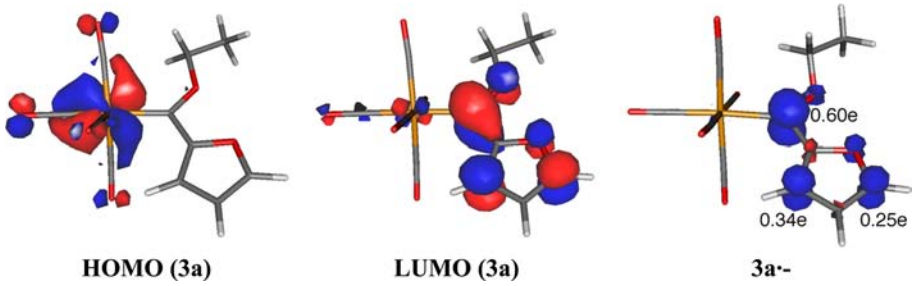

Figure 7. Frontier Molecular Orbitals of **3a** and computed spin density on **3a**•⁻.

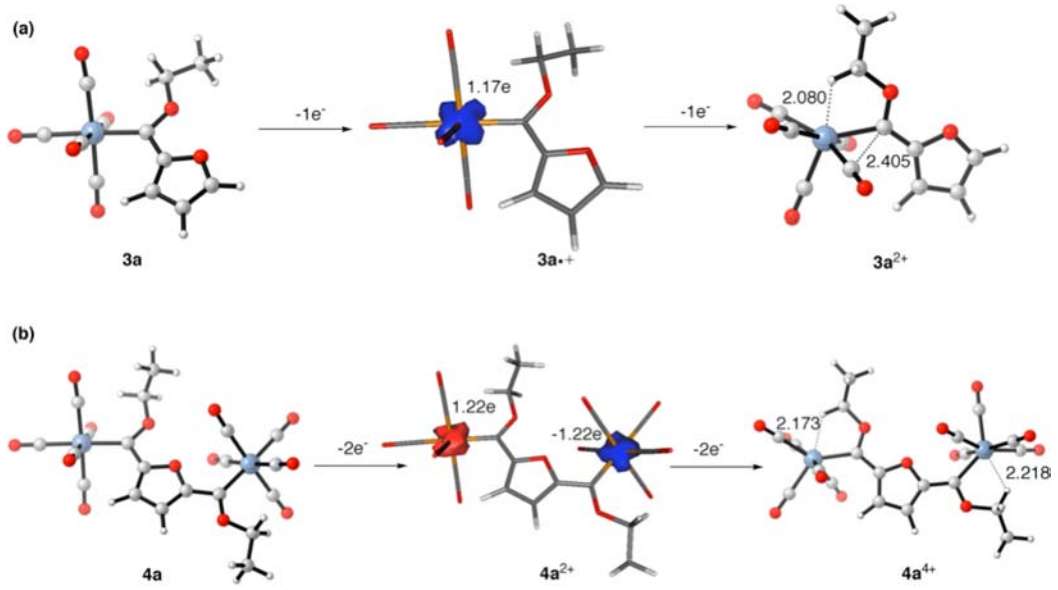

Figure 8. Species formed upon electrochemical oxidation processes of complexes **3a** (a) and **4a** (b). Bond lengths are given in angstroms.

NMR study discussed above, showing that the Cr=C functionality of furyl complexes were more shielded than thienyl complexes.

Upon changing the OEt substituent to NHBu to give $[(OC)_5Cr{=}C(NHBu)Ar]$, the same trend was observed in that **5b** (Ar = Th) is also reduced at an E_{pc} 105 mV larger than **5a** (Ar = Fu). (There was no E_{pa} observed for **5a** implying $\Delta E^{\circ\prime}$ could not be calculated). Both the NHBu and OEt groups are directly bonded to the Cr=C center and, like the aryl groups, also allow for conjugation (Figures 1 and 2). The NHBu group shifted the formal reduction potential of the Cr=C species with $\Delta E_{pc} = E_{pc,Fu\text{-}OEt,\mathbf{3a}} - E_{pc,Fu\text{-}NHBu,\mathbf{5a}} = -1823 - (-2398) =$ 575 mV and $\Delta E^{\circ\prime} = E^{\circ\prime}_{Th\text{-}OEt,\mathbf{3b}} - E^{\circ\prime}_{Th\text{-}NHBu,\mathbf{5b}} =$ 470 mV to more negative potentials than those observed for OEt derivatives, in agreement with the computed less negative LUMO energies (−2.16 and −2.20 eV for **5a** and **5b**, respectively). Clearly, from these large shifts to more negative potentials, the NHBu group is more successful in donating electrons to the Cr=C redox center (Figure 2) than the OEt functionality, which agrees with the well-known higher donor-ability of nitrogen atoms compared to the more electronegative oxygen atoms.

The changes in Cr=C reduction potential as a function of Ar, OEt, or NHBu for the biscarbenes was not as large, but in essence the same general directional changes in potentials were observed. The observed shifts in potentials as a function of aryl, OEt, and NHBu functionalities are summarized in Figure 6. The only biscarbene Cr=C reduction that could not be interpreted within this context was **6b** since this redox process ($E_{pc} < -2.4$ V) fell outside the potential window of the solvent CH_2Cl_2.

Cr(0) oxidation to Cr(I) is observed in the potential range $0.289 < E^{\circ\prime} < 0.650$ V (Table 3). As shown in Figure 7, the HOMO of furyl complex **3a** is mainly located at the chromium(0) atom.[34] Similar HOMOs were observed for the rest of the complexes. Thus, the first oxidation process in all complexes may be attributed to the one-electron oxidation of Cr(0) to Cr(I) which leads to a radical cation where the unpaired electron is located in the transition metal atom (see also Figure 8). For the biscarbene complexes **2**, **4**, and **6** the oxidation of the two Cr(0) centers takes place at such closely overlapping potentials that, with the exception of **2** (Table 3), they could not be resolved. Hence in the computational discussion of **4a** below, this oxidation was modeled as a process in which two electrons were transferred simultaneously. The $Cr^{0/1}$ redox couple has better ΔE_p values than Cr=C reduction with the ethoxy biscarbenes **4a** (Ar = Fu) and **4b** (Ar = Th) as well as the amino monocarbene **5a** showing $\Delta E_p < 69$ mV, but by and large this couple was also electrochemically pseudo reversible. Peak current ratios were better than 0.69 for almost all mono- and bis-Fu and Th complexes. The monomeric Fu and Th NHBu complexes **5a** and **5b** showed splitting of the $Cr^{0/1}$ couple into poorly resolved components a and b (Figures 5 and 6, Table 3), which is consistent with the rotamers shown in Figure 2. From NMR measurements, see above, the *syn* and *anti* zwitterionic rotamers are present in an approximate ratio of

dx.doi.org/10.1021/ic4007422 | Inorg. Chem. 2013, 52, 6674−6684

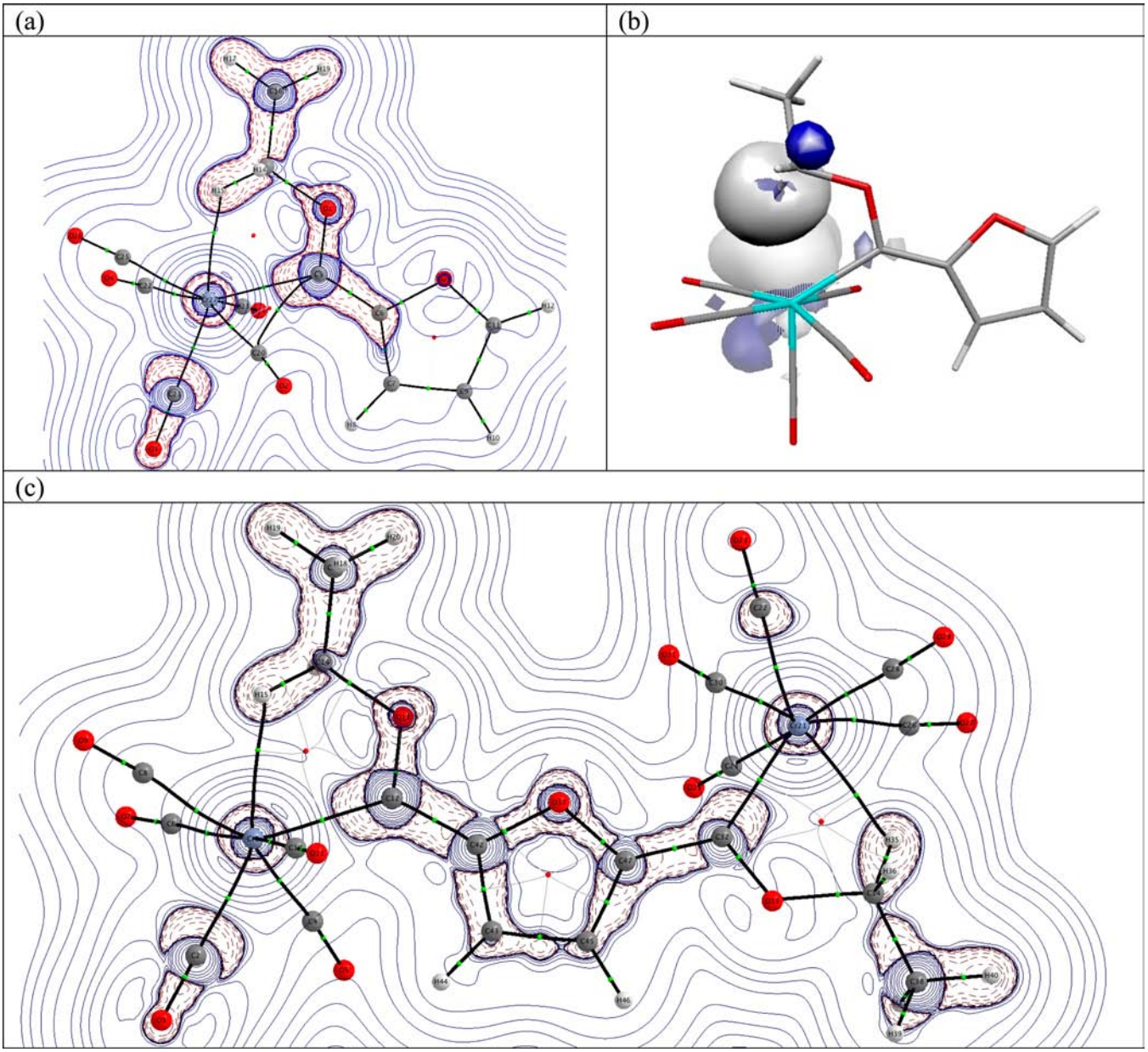

Figure 9. Contour line diagrams $\nabla^2\rho(r)$ for complexes $\mathbf{3a}^{2+}$ (a) and $\mathbf{4a}^{4+}$ (c) in the Cr−H−C plane. Solid lines indicate areas of charge concentration ($\nabla^2\rho(r) < 0$) while dashed lines show areas of charge depletion ($\nabla^2\rho(r) > 0$). The solid lines connecting the atomic nuclei are the bond paths while the small red spheres indicate the corresponding bond critical points. The solid lines separating the atomic basins indicate the zero-flux surfaces crossing the molecular plane. (b) NBO orbitals associated with the σ(C−H) → d(Cr) agostic interaction.

1:1. The oxidation of one of the zwitterionic rotamers of **5a** and **5b** is associated with one of the two $Cr^{0/1}$ peaks, while the other $Cr^{0/1}$ peak may be associated with the other zwitterionic species shown in Figure 2.

As with reduction wave I, the potentials associated with Cr(0) oxidation of [(OC)$_5$Cr═C(NHBu)Ar] for the Ar = Fc complex **1** (0.289 V) and the two NHBu complexes **5a** and **5b** were the lowest (Figure 6, Table 3). The ethoxy-furan carbene **3a** exhibited a Cr(0) oxidation potential 209 mV more positive than **1** (compared to the 265 mV more positive potential observed for Cr═C reduction) while the thienyl derivative is, as with Cr═C reduction, oxidized at the largest potential. $\Delta E^{\circ\prime} = E^{\circ\prime}_{\mathbf{Th,3b}} - E^{\circ\prime}_{\mathbf{Fu,3a}}$ was 67 mV for wave 1 while for Cr═C reduction the corresponding potential shift was 121 mV. The thienyl butylamino derivative **5b** also undergoes Cr(0) oxidation at a formal oxidation potential 33 mV more positive (wave 1b) than the furan derivative **5a**. Again, a clear correlation between the observed first oxidation potential and the computed HOMO energies can be found: −5.70 eV (**5b**) < 5.84 eV (**1**) < −5.94 (**3a**) < −5.96 eV (**3b**), thus showing that a more stabilized HOMO (i.e., more negative) is translated into a higher oxidation potential. In comparison to the OEt substituent, the NHBu functionality shifted the formal oxidation potential of the Cr(0) species with $\Delta E^{\circ\prime}_{\mathrm{Cr0/1}} = E^{\circ\prime}_{\mathbf{Fu\text{-}OEt,3a}} - E^{\circ\prime}_{\mathbf{Fu\text{-}NHBu,5a}} = 96$ mV and $\Delta E^{\circ\prime} = E^{\circ\prime}_{\mathbf{Th\text{-}OEt,3b}} - E^{\circ\prime}_{\mathbf{Th\text{-}NHBu,5b}} = 130$ mV (utilizing wave 1b for **5a** and **5b**) to more negative potentials (Table 3, Figure 6). Although this shift is less than that observed for Cr═C reduction, the shift was in the same direction and thus mutually consistent with the conclusion that the NHBu group are more successful in

dx.doi.org/10.1021/ic4007422 | Inorg. Chem. 2013, 52, 6674−6684

donating electrons to the Cr=C redox center than the OEt functionality.

Finally, at the positive edge of the potential window of CH_2Cl_2, we could observe a second, irreversible (i_{pc} = 0) oxidation process for **3b**, **4a**, **4b**, and **6a**. For all other complexes this redox process fell outside the workable potential window of CH_2Cl_2. This second observed oxidation process at wave 2 (Figure 4) belongs to Cr(I) oxidation to Cr(II) because the unpaired electron in the corresponding radical cation is located in the metal atom (see Figure 8a). As the $Cr^{I/II}$ couple is electrochemically irreversible, and because the observed, quite similar, E_{pa} values (Figure 6) are so close to the edge of the solvent potential window, it was not possible to interpret any potential changes as a function of carbene substituents. The complete irreversibility of the $Cr^{I/II}$ couple with i_{pc}/i_{pa} = 0 (wave 2, Figure 4, Table 3) contrasts the Cr=C reduction (wave I) which exhibited in most cases nonzero i_{pa}/i_{pc} ratios. This highlights that the electrochemically generated Cr(II) species is much more reactive than the electrochemically generated $^{-}$Cr−C• species, and destructs on a much faster time scale.

The latter result prompted us to analyze the nature of the dicationic species formed upon the second electrochemical oxidation process in detail. As is readily seen in Figure 8a, dicationic complex $\mathbf{3a}^{2+}$ exhibits an unusual structure which is markedly different to the structures of **3a** and the radical cation $\mathbf{3a}^{\bullet+}$. Indeed, a hydrogen atom of the ethoxy moiety is found close to the chromium atom (Cr···H distance of 2.080 Å), pointing to a possible C−H agostic interaction.

To gain more insight into the bonding situation of $\mathbf{3a}^{2+}$, we also analyzed the C−H···Cr interaction with the help of the Atom in Molecules (AIM)[35] and Natural Bond Orbital (NBO)[36] methods. The laplacian distribution of $\mathbf{3a}^{2+}$ in the Cr···H−C plane (Figure 9a) clearly reveals the occurrence of a bond critical point located at the midpoint between the transition metal and the hydrogen atom, which is associated with a bond path running between the corresponding two atoms. This proves the existence of a direct interaction between both atoms. Moreover, the computed value of 0.035 e $Å^{-3}$ for the electron density at the bond critical point is in the range expected for CH agostic interactions.[37] This is further supported by the NBO method which locates a stabilizing electronic donation from the doubly occupied σ(C−H) molecular orbital to the vacant d atomic orbital of the chromium (associated second-order perturbation energy of −36.7 kcal/mol, see Figure 9b). The presence of the vacant orbital is, of course, a direct consequence of the oxidation process which eliminates the two electrons present in the HOMO of **3a** (located in the chromium atom). The special bonding situation of $\mathbf{3a}^{2+}$ seems to be general as a similar structure was found for the tetracationic species $\mathbf{4a}^{4+}$ formed upon two consecutive two-electron oxidation processes from **4a** via the open-shell singlet species $\mathbf{4a}^{2+}$ (see Figures 8b and 9c).

Finally, with respect to the furyl- and thienyl-containing butylamino monocarbene complexes **5a** and **5b**, Scheme 2 highlights the electrochemical pathway of the observed redox processes. The ethoxy monocarbene complexes undergo essentially the same processes while for the biscarbenes complexes a second $^{-}$Cr−C• radical anion, Cr(0) and Cr(I) oxidation at overlapping potentials with the first processes at waves I, **1** and **2** (Figure 4) also form.

Scheme 2. Electrochemical Reactions Associated with 5a (Ar = Fu) and 5b (Ar= Th)[a]

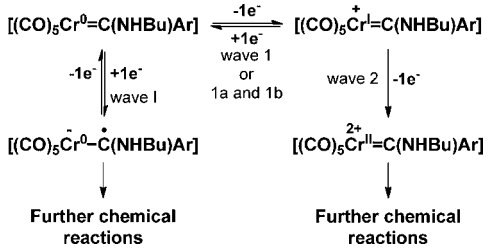

[a]Both the final reduction product possessing the $^{-}$Cr−C• radical anion and the final oxidation product possessing the Cr(II) centre are highly reactive and undergo further chemical decomposition reactions.

CONCLUSIONS

New furyl mono- and bis-butylaminocarbene chromium complexes [(CO)$_5$Cr=C(NHBu)Fu], **5a**, and [(CO)$_5$Cr=C(NHBu)-Fu′-(NHBu)C=Cr(CO)$_5$], **6a**, were prepared from the ethoxy precursors. The formation of both *syn*- and *anti*-rotamers across the restricted $C_{carbene}$−N bond was observed by the duplication of all ^{1}H NMR signals of **5a** in a ratio of 1:0.95 (*syn*:*anti*). Ferrocenyl and thienyl derivatives were also prepared, and the structure of **4a** [(CO)$_5$Cr=C(OEt)-Fu′-(OEt)C=Cr(CO)$_5$] was solved. From an electrochemical study it was found that the carbene functionality of all ferrocenyl substituted complexes were most electron-rich but that the Cr=C functionality of thienyl complexes were most electron-poor. This result is mutually consistent with a ^{13}C NMR study that showed the Cr=C functionality of furyl complexes were more shielded than thienyl complexes. Three carbene-based redox processes were observed: electrochemical pseudo reversible reduction of Cr=C to $^{-}$Cr−C• at far negative (<1.7 V vs FcH/FcH^+) potentials, electrochemical pseudo reversible oxidation of Cr(0) to Cr(I) at 0.29−0.65 V, and irreversible oxidation of Cr(I) to Cr(II) at the positive edge of the solvent (CH_2Cl_2) potential window. The ferrocenyl group is oxidized at potentials between that of the $Cr^{0/I}$ and the $Cr^{I/II}$ couple. These redox assignments were mutually consistent with the computational data obtained at the DFT level, which suggest a peculiar bonding situation in the species formed upon the second oxidation process (i.e., stabilized by CH···Cr agostic interactions). Poorly resolved peak splitting of the Cr(0) oxidation of the zwitterionic species [(OC)$_5$Cr^{-}—C=(N^{+}BuH)Ar], Ar = Fu or Th into a and b components is consistent with the presence of *syn*- and *anti*-rotamers across the restricted $C_{carbene}$−N bond.

EXPERIMENTAL SECTION

General Considerations. All operations were carried out under an inert atmosphere of nitrogen or argon gas using standard Schlenk techniques. Solvents were dried by refluxing on sodium metal (hexane, thf, and diethylether) or over phosphorus pentoxide (CH_2Cl_2) and then distilled under nitrogen prior to use. Chemicals were used without further purification unless stated otherwise. Triethyloxonium tetrafluoroborate (Et_3OBF_4) was synthesized according to literature procedures.[15] Purification with column chromatography was done using silica gel 60 (0.0063−0.200 mm) as stationary phase. A Bruker AVANCE 500 spectrometer was used for NMR recordings. ^{1}H NMR spectra were recorded at 500.139 MHz and ^{13}C NMR spectra at 125.75 MHz. The signal of the solvent was used as reference: ^{1}H $CDCl_3$ at 7.24 ppm and ^{13}C $CDCl_3$ at 77.00 ppm. Solution IR spectra were recorded on a Perkin-Elmer Spectrum RXI FT-IR spectrophotometer using hexane as solvent. Only the vibration bands in the

dx.doi.org/10.1021/ic4007422 | Inorg. Chem. 2013, 52, 6674−6684

carbonyl-stretching region (ca. 1600−2200 cm^{-1}) were recorded. Melting points were not recorded because of decomposition during heating.

Synthesis of Carbene Complexes 1−4. The carbene complexes **1**,[16] **2**,[18] **3**,[17] **4a**,[4e] **4b**,[4f] **5b**[7] and **6b**[7] were prepared according to known literature procedures. Spectroscopic data for **1**, **2**, **3b**, **4b**, **5b**, and **6b** have been reported in our previous study.[7]

[Cr(CO)$_5${C(OEt)Fu}] ***3a.***[17] ^{1}H NMR ($CDCl_3$, δ/ppm): 7.82 (dd, J = 1.6, 0.8 Hz, 1H, Fu-H_γ), 6.96 (dd, J = 3.6, 0.8 Hz, 1H, Fu-H_α), 6.56 (dd, J = 3.6, 1.6 Hz, 1H, Fu-H_β), 5.13 (q, J = 7.0 Hz, 2H, OCH_2), 1.63 (t, J = 7.0 Hz, 3H, CH_3); ^{13}C NMR ($CDCl_3$, δ/ppm): 311 ($C_{carbene}$), 224 (CO_{trans}), 217 (CO_{cis}), 164 (Fu-C_{ipso}), 150 (Fu-C_γ), 113 (Fu-C_β), 112 (Fu-C_α), 76 (OCH_2), 15 (CH_3). IR (hexane, ν(CO)/cm^{-1}): 2061 s (A''_1), 1990 w (B), 1960 s (A'_1), 1946 vs (E).

[(CO)5Cr{C(OEt)(Fu′)C(OEt)}Cr(CO)5] ***4a.***[4e] ^{1}H NMR ($CDCl_3$, δ/ppm): 7.22 (s, 2H, Fu′-$H_{\alpha,\alpha'}$), 5.22 (q, 4H, J = 7.0 Hz, OCH_2), 1.72 (t, 6H, J = 7.1 Hz, CH_3); ^{13}C NMR ($CDCl_3$, δ/ppm): 313 ($C_{carbene}$), 224 (CO_{trans}), 216 (CO_{cis}), 162 (Fu′-C_{ipso}), 119 (Fu′-$C_{\alpha,\alpha'}$), 77 (OCH_2), 15 (CH_3). IR (hexane, ν(CO)/cm^{-1}): 2054 s (A''_1), 1995 w (B), 1962 s (A'_1), 1955 vs (E).

Synthesis of New Furyl Aminocarbene Complexes 5a and 6a. *[Cr(CO)$_5${C(NHBu)Fu}]* ***5a.*** **3a** (2 mmol, 0.69 g) was dissolved in ether and *n*-butylamine (2.2 mmol, 0.22 mL) was added at room temperature (rt). A rapid color change from red to yellow was observed. Volatiles were removed by reduced pressure, and purification was done using column chromatography with a 1:1 hexane/CH_2Cl_2 solvent mixture. Two isomers formed and although it could not be separated by column chromatography, two sets of NMR data could be distinguished. Yield 0.55g (85%) yellow crystals.

Syn-Isomer. ^{1}H NMR ($CDCl_3$, δ/ppm): 9.22 (br, 1H, NH), 7.44 (d, J = 1.7 Hz, 1H, Fu-H_γ), 7.09 (d, J = 3.6 Hz, 1H, Fu-H_α), 6.57 (dd, 3.5, 1.9 Hz, 1H, Fu-H_β), 4.06 (td, 7.2, 6.0 Hz, 2H, NCH_2), 1.80 (m, 2H, CH_2CH_2), 1.50 (m, 2H, CH_2CH_2), 0.98 (t, 7.4 Hz, 3H, CH_3); ^{13}C NMR ($CDCl_3$, δ/ppm): 243 ($C_{carbene}$), 223 (CO_{trans}), 218 (CO_{cis}), 157 (Fu-C_{ipso}), 144 (Fu-C_γ), 122 (Fu-C_α), 114 (Fu-C_β), 53 (NCH_2), 32 (CH_2CH_2), 20 (CH_2CH_2), 14 (CH_3).

Anti-Isomer. ^{1}H NMR ($CDCl_3$, δ/ppm): 8.28 (br, 1H, NH), 7.67 (d, J = 1.4 Hz, 1H, Fu-H_γ), 7.44 (d, J = 3.7 Hz, 1H, Fu-H_α), 6.59 (dd, 3.6, 1.7 Hz, 1H, Fu-H_β), 3.70 (td, 7.1, 5.6 Hz, 2H, NCH_2), 1.76(m, 2H, CH_2CH_2), 1.45 (m, 2H, CH_2CH_2), 1.01 (t, 7.4 Hz, 3H, CH_3). ^{13}C NMR ($CDCl_3$, δ/ppm): 250 ($C_{carbene}$), 223 (CO_{trans}), 218 (CO_{cis}), 156 (Fu-C_{ipso}), 146 (Fu-C_γ), 125 (Fu-C_α), 113 (Fu-C_β), 53 (NCH_2), 32 (CH_2CH_2), 20 (CH_2CH_2), 14 (CH_3). IR (hexane, ν(CO)/ cm^{-1}) 2055 m (A_1''), 1971 vw (B), 1910 m (A_1'), 1935 vs (E).

[(CO)$_5$Cr{C(NHBu)(Fu′)C(NHBu)}Cr(CO)$_5$] ***6a.*** **4a** (2 mmol, 1.24 g) was dissolved in ether and *n*-butylamine (4.2 mmol, 0.42 mL) was added at rt. The color changed from purple to deep yellow, and volatiles were removed under reduced pressure. Yield 0.98g (75%) orange crystals.

Syn,syn-Isomer. ^{1}H NMR ($CDCl_3$, δ/ppm): 9.12 (br, 1H, NH), 7.13 (s, 2H, Fu′-$H_{\alpha,\alpha'}$), 4.12 (dd, J = 7.1, 6.7 Hz, 4H, NCH_2), 1.88−1.76 (m, 4H, CH_2CH_2), 1.59−1.48 (m, 4H, CH_2CH_2), 0.91 (t, J = 7.3 Hz, 6H, CH_3); ^{13}C NMR ($CDCl_3$, δ/ppm): 250 ($C_{carbene}$) 223 (CO_{trans}), 218 (CO_{cis}), 159(C_{ipso}), 118 (Fu′-$C_{\alpha,\alpha'}$), 52 (NCH_2), 31 (CH_2CH_2), 20 (CH_2CH_2), 14 (CH_3). IR (hexane, ν(CO)/cm^{-1}): 2053 m (A_1''), 1975 vw (B), 1916 m (A_1'), 1936 vs (E).

Crystal Structure Determination. Data for a dark-purple needle crystal (0.018 × 0.020 × 0.376 mm) of **4a** were collected at 150 K on a Bruker D8 Venture kappa geometry diffractometer, with duo Iμs sources, a Photon 100 CMOS detector, and APEX II[38] control software using Quazar multilayer optics monochromated, Mo-$K\alpha$ radiation by means of a combination of ϕ and ω scans. Data reduction was performed using SAINT+,[38] and the intensities were corrected for absorption using SADABS.[38] The structure was solved by intrinsic phasing using SHELXTS[39] and refined by full-matrix least-squares using SHELXTL[39] and SHELXL-2012.[39] In the structure refinement all hydrogen atoms were added in calculated positions and treated as riding on the atom to which they are attached. All non-hydrogen atoms were refined with anisotropic displacement parameters, all isotropic displacement parameters for hydrogen atoms were calculated as X × U_{eq} of the atom to which they are attached, X = 1.5 for the methyl hydrogens and 1.2 for all other hydrogens. One methyl group in each molecule (C16, C36) is disordered, and two sites were refined for each (in both cases with a refined sof ratio of 0.61: 0.39). The major site for C16 (C16A) is shown in Figure 3.

Electrochemical Studies. CVs, square wave voltammograms (SWs), and linear sweep voltammograms (LSVs) were recorded on a Princeton Applied Research PARSTAT 2273 voltammograph running PowerSuite (Version 2.58) utilizing a standard three-electrode cell in a M Braun Lab Master SP glovebox filled with high purity argon (H_2O and O_2 < 5 ppm). A platinum wire auxiliary electrode, a silver wire pseudo internal reference, and a glassy carbon working electrode (surface area 3.14 mm^2) was utilized after polishing on a Buhler polishing mat first with 1 μm and then with 1/4 μm diamond paste. All electrode potentials are reported versus the ferrocene/ferrocenium redox couple (FcH/FcH$^+$, FcH = Fe(η^5-C_5H_5)$_2$, $E^{\circ\prime}$ = 0.00 V) as reference.[40] However, decamethylferrocene, Fc*, was used as internal standard to prevent signal overlap with the ferrocenyl of **1** and **2**. Decamethylferrocene has a potential of −550 mV versus free ferrocene with ΔE = 72 mV and i_{pc}/i_{pa} = 1 under the conditions employed.[41] Analyte solutions (0.5 mmol dm^{-3}) were prepared in dry CH_2Cl_2 in the presence of 0.1 mol dm^{-3} [(nBu$_4$)N][PF_6]. Analyses were performed at 20 °C. Data were exported to a spread sheet program for manipulation and diagram preparation.

Computational Studies. Geometry optimizations without symmetry constraints were carried out using the Gaussian09 suite of programs[42] at the B3LYP (uB3LYP for open-shell species)[43] using the double-ζ plus polarization def2-SVP[44] basis set for all atoms. This protocol is denoted B3LYP/def2-SVP. All species were characterized by frequency calculations, and have a positive defined Hessian matrix indicating that they are minima on the potential energy surface. Donor−acceptor interactions were computed using the natural bond orbital (NBO) method.[34] The energies associated with these two-electron interactions have been computed according to the following equation:

$$\Delta E^{(2)}_{\phi\phi^*} = -n_\phi \frac{\langle \phi|\hat{F}|\phi\rangle^2}{\varepsilon_{\phi^*} - \varepsilon_\phi}$$

where F is the DFT equivalent of the Fock operator and ϕ and ϕ^* are two filled and unfilled Natural Bond Orbitals having ε_ϕ and ε_{ϕ^*} energies, respectively; n_ϕ stands for the occupation number of the filled orbital.

The AIM[33] results described in this work correspond to calculations performed at the B3LYP/def2-SVP level on the optimized geometries. The topology of the electron density was studied using the AIMAll program package.[45]

■ ASSOCIATED CONTENT

Ⓢ Supporting Information

The Cartesian coordinates and energies for the optimized compounds **3a** and **4a** and the corresponding radical ions. X-ray crystallographic data on **4a** in CIF format. This material is available free of charge via the Internet at http://pubs.acs.org.

■ AUTHOR INFORMATION

Corresponding Author

*E-mail: daniela.bezuidenhout@up.ac.za (D.I.B.), israel@quim.ucm.es (I.F.). Fax: +27-(0)12-420-4687 (D.I.B.). Phone: +27-(0)12- 420-2626 (D.I.B.), +34-913944310 (I.F.).

Author Contributions

The manuscript was written through contributions of all authors. All authors have given approval to the final version of the manuscript.

Notes

The authors declare no competing financial interest.

■ ACKNOWLEDGMENTS

This work is supported by the National Research Foundation, South Africa (D.I.B., Grant 76226; J.C.S., Grant 81829), and the Spanish MINECO and CAM (I.F., Grants CTQ2010-20714-CO2-01/BQU, Consolider-Ingenio 2010, CSD2007-00006, S2009/PPQ-1634).

■ REFERENCES

(1) Fischer, E. O.; Maasböl, A. *Angew. Chem.* **1964**, *3b*, 645.
(2) (a) Mills, O. S.; Redhouse, A. D. *J. Chem. Soc. A* **1968**, 642−647. (b) Fischer, E. O. *Angew. Chem.* **1974**, *86*, 651−663.
(3) Representative examples: (a) Cases, M.; Frenking, G.; Duran, M.; Solà, M. *Organometallics* **2002**, *21*, 4182−4191. (b) Poater, J.; Cases, M.; Fradera, X.; Duran, M.; Solà, M. *Chem. Phys.* **2003**, *294*, 129−139. (c) Frenking, G.; Solà, M.; Vyboishchikov, S. F. *J. Organomet. Chem.* **2005**, *690*, 6178−6204. (d) Lage, M. L.; Fernández, I.; Mancheño, M. J.; Sierra, M. A. *Inorg. Chem.* **2008**, *47*, 5253−5258. (e) Valyaev, D. A.; Brousses, R.; Lugan, N.; Fernández, I.; Sierra, M. A. *Chem.—Eur. J.* **2011**, *17*, 6602−6605. (f) Lugan, N.; Fernández, I.; Brousses, R.; Valyaev, D. A.; Lavigne, G.; Ustynyukd, N. A. *Dalton Trans.* **2013**, *42*, 898−901.
(4) (a) For a recent review, see: Bezuidenhout, D. I.; Lotz, S.; Liles, D. C.; van der Westhuizen, B. *Coord. Chem. Rev.* **2012**, *256*, 479−524. (b) Lotz, S.; van Jaarsveld, N. A.; Liles, D. C.; Crause, C.; Gorls, H.; Terblans, Y. M. *Organometallics* **2012**, *31*, 5371−5383. (c) Bezuidenhout, D. I.; Lotz, S.; Landman, M.; Liles, D. C. *Inorg. Chem.* **2011**, *50*, 1521−1533. (d) Bezuidenhout, D. I.; Barnard, W.; van der Westhuizen, B.; van der Watt, E.; Liles, D. C. *Dalton Trans.* **2011**, *40*, 6711−6727. (e) Crause, C.; Gorls, H.; Lotz, S. *Dalton Trans.* **2005**, 1649−1657. (f) Terblans, Y. M.; Roos, H. M.; Lotz, S. *J. Organomet. Chem.* **1998**, *566*, 133−142.
(5) (a) Lotz, S.; Crause, C.; Olivier, A. J.; Liles, D. C.; Gorls, H.; Landman, M.; Bezuidenhout, D. I. *Dalton Trans.* **2009**, 697−710. (b) Landman, M.; Ramontja, J.; van Staden, M.; Bezuidenhout, D. I.; van Rooyen, P. H.; Liles, D. C.; Lotz, S. *Inorg. Chim. Acta* **2010**, *363*, 705−717. (c) Chu, G. M.; Fernández, I.; Sierra, M. A. *Chem.—Eur. J.* **2013**, *19*, 5899−5908.
(6) (a) Auger, A.; Muller, A. J.; Swarts, J. C. *Dalton Trans.* **2007**, 3623−3633. (b) Cook, M. J.; Chambrier, I.; White, G. F.; Fourie, E.; Swarts, J. C. *Dalton Trans.* **2009**, 1136−1144. (c) Conradie, J.; Cameron, T. S.; Aquino, M. A. S.; Lamprecht, G. J.; Swarts, J. C. *Inorg. Chim. Acta* **2005**, *358*, 2530−2542.
(7) Van der Westhuizen, B.; Swarts, P. J.; Strydom, I.; Liles, D. C.; Fernández, I.; Swarts, J. C.; Bezuidenhout, D. I. *Dalton Trans.* **2013**, *42*, 5367−5378.
(8) (a) Pombeiro, A. J. L. *New J. Chem.* **1997**, *21*, 649−660. (b) Casey, C. P.; Albin, L. D.; Saeman, M. C.; Evans, D. H. *J. Organomet. Chem.* **1978**, *155*, C37−C40. (c) Limberg, A.; Lemos, M. A. N. D. A.; Pombeiro, A. J. L.; Maiorana, S.; Papagni, A.; Licandro, E. *Port. Electrochim. Acta* **1995**, *13*, 319−323. (d) Lloyd, M. K.; McCleverty, J. A.; Orchard, D. G.; Connor, J. A.; Hall, M. B.; Hillier, I. H.; Jones, E. M.; McEwen, G. K. *J. Chem. Soc., Dalton Trans.* **1973**, 1743−1747.
(9) (a) Fernández, I.; Mancheño, M. J.; Gómez-Gallego, M.; Sierra, M. A. *Org. Lett.* **2003**, *5*, 1237−1240. (b) Martínez-Álvarez, R.; Gómez-Gallego, M.; Fernández, I.; Mancheño, M. J.; Sierra, M. A. *Organometallics* **2004**, *23*, 4647−4654. (c) Wulff, W. D.; Korthals, K. A.; Martínez-Álvarez, R.; Gómez-Gallego, M.; Fernández, I.; Sierra, M. A. *J. Org. Chem.* **2005**, *70*, 5269−5277. (d) López-Alberca, M. P.; Mancheño, M. J.; Fernández, I.; Gómez-Gallego, M.; Sierra, M. A.; Hemmert, C.; Gornitzka, K. H. *Eur. J. Inorg. Chem.* **2011**, 842−849.
(10) Selected recent reviews on the chemistry and applications of Fischer carbenes: (a) Wu, Y.-T.; Kurahashi, T.; de Meijere, A. *J. Organomet. Chem.* **2005**, *690*, 5900−5911. (b) Gómez-Gallego, M.; Mancheño, M. J.; Sierra, M. A. *Acc. Chem. Res.* **2005**, *38*, 44−53. (c) Sierra, M. A.; Gómez-Gallego, M.; Martínez-Ávarez, R. *Chem.−Eur. J.* **2007**, *13*, 736−744. (d) Sierra, M. A.; Fernández, I.; Cossío, F. P. *Chem. Commun.* **2008**, 4671−4682. (e) Dötz, K. H.; Stendel, J. *Chem. Rev.* **2009**, *109*, 3227−3274. (f) Herndon, J. W. *Coord. Chem. Rev.* **2010**, *254*, 103−194. (g) Fernández-Rodríguez, M. A.; García-García, P.; Aguilar, E. *Chem. Commun.* **2010**, *46*, 7670−7687. (h) Fernández, I.; Cossío, F. P.; Sierra, M. A. *Acc. Chem. Res.* **2011**, *44*, 479−490.
(11) (a) Baldoli, C.; Cerea, P.; Falciola, L.; Giannini, C.; Licandro, F.; Maiorana, S.; Mussini, P.; Perdiccia, D. *J. Organomet. Chem.* **2005**, *690*, 5777−5787. (b) Hoskovcova, I.; Zverinova, R.; Rohacova, J.; Dvorak, D.; Tobrman, T.; Zalis, S.; Ludvik. *J. Electrochim. Acta* **2011**, *56*, 6853−6859. (c) Hoskovcova, I.; Rohacova, J.; Dvorak, D.; Tobrman, T.; Zalis, S.; Zverinova, R.; Ludvik. *J. Electrochim. Acta* **2010**, *55*, 8341−8351. (d) Pombeiro, A. J. L. *J. Organomet. Chem.* **2005**, *690*, 6021−6040. (e) Hoskovcova, I.; Rohacova, J.; Meca, L.; Tobrman, T.; Dvorak, D.; Ludvik. *J. Electrochim. Acta* **2005**, *50*, 4911−4915. (f) Raubenheimer, H. G.; du Toit, A.; du Toit, M.; An, J.; van Niekerk, L.; Cronje, S.; Esterhuysen, C.; Crouch, A. M. *Dalton Trans.* **2004**, 1173−1180.
(12) (a) Bernasconi, C. F.; Ali, M.; Lu, F. *J. Am. Chem. Soc.* **2000**, *122*, 1352−1359. (b) Dötz, K. H. *Angew. Chem., Int. Ed. Engl.* **1975**, *14*, 644−645.
(13) (a) Connor, J. A.; Jones, E. M.; Randall, E. W.; Rosenburg, E. *J. Chem. Soc., Dalton Trans.* **1972**, *22*, 2419. (b) Connor, J. A.; Jones, E. M. *J. Chem. Soc. A* **1971**, *12*, 1974−1979.
(14) While writing this paper, the authors became aware of an independent but simultaneously conducted electrochemical study of related but different chromium carbene complexes, see Metelkova, R.; Tobrman, T.; Kvapilova, H.; Hoskovcova, I.; Ludvik, J. *Electrochim. Acta* **2012**, *82*, 470−477.
(15) Meerwein, H. *Org. Synth.* **1966**, *46*, 113−115.
(16) Lopez-Cortez, J. G.; de la Cruz, L. F. C.; Ortega-Alfaro, M. C.; Toscano, R. A.; Alvarez-Toledano, C.; Rudler, H. *J. Organomet. Chem.* **2005**, *690*, 2229−2237.
(17) (a) Aoki, S.; Fujimura, T.; Nakamura, E. *J. Am. Chem. Soc.* **1992**, *114*, 2985. (b) Connor, J. A.; Lloyd, J. P. *J. Chem. Soc., Dalton Trans.* **1972**, 1470−1476.
(18) (a) Bezuidenhout, D. I.; van der Watt, E.; Liles, D. C.; Landman, M.; Lotz, S. *Organometallics* **2008**, *27*, 2447−2456. (b) Connor, J. A.; Jones, E. M.; Lloyd, J. P. *J. Organomet. Chem.* **1970**, *24*, C20−C22.
(19) (a) Bezuidenhout, D. I.; Liles, D. C.; van Rooyen, P. H.; Lotz, S. *J. Organomet. Chem.* **2007**, *692*, 774−783. (b) Klabunde, U.; Fischer, E. O. *J. Am. Chem. Soc.* **1967**, *89*, 7141−7142.
(20) For a definition of *syn/anti* conformers, see: (a) Fernández, I.; Cossío, F. P.; Arrieta, A.; Lecea, B.; Mancheño, M. J.; Sierra, M. A. *Organometallics* **2004**, *23*, 1065−1071. (b) Andrada, D. M.; Zoloff Michoff, M. E.; Fernández, I.; Granados, A. M.; Sierra, M. A. *Organometallics* **2007**, *26*, 5854−5858. See also references 3e and 3f.
(21) Pretch, E.; Seibl, J.; Clerc, T.; Simon, W. *Tables for Spectral Data for Structure Determination of Organic Compounds*, 2nd ed.; Springer-Verlag: Berlin, Germany, 1989.
(22) (a) Post, E. W.; Watters, K. L. *Inorg. Chim. Acta* **1978**, *26*, 29−36. (b) Moser, E.; Fischer, E. O. *J. Organomet. Chem.* **1968**, *15*, 147−155.
(23) (a) Braterman, P. S. *Metal Carbonyl Spectra*; Academic Press Inc.: London, U.K., 1975; p 68; (b) Adams, D. M. *Metal−Ligand and Related Vibrations*; Edward Arnold Publishers Ltd: London, U.K., 1967; p 98.
(24) Liles, D. C.; Lotz, S. *Acta Crystallogr.* **2006**, *E62*, m331−m334.
(25) (a) Faruggia, L. J. *J. Appl. Crystallogr.* **1997**, *30*, 565. (b) Cason, C. J. *POV-RAY for Windows*, Persistence of Vision, 2004.
(26) Richardson, D. E.; Taube, H. *Inorg. Chem.* **1981**, *20*, 1278−1285.
(27) (a) Fry, A. J. *Synthetic Organic Electrochemistry*, 2nd ed., John Wiley and Sons,: New York, 1989; p 208, 232; (b) Volke, J.; Liska, F. *Electrochemistry in Organic Synthesis*; Springer-Verlag: Berlin, Germany, 1994; p 90.
(28) (a) Gericke, H. J.; Barnard, N. I.; Erasmus, E.; Swarts, J. C.; Cook, M. J.; Aquino, M. A. S. *Inorg. Chim. Acta* **2010**, *363*, 2222−2232. (b) Evans, D. H.; OConnell, K. M.; Peterson, R. A.; Kelly, M. J. *J. Chem. Educ.* **1983**, *60*, 290−293. (c) Kissinger, P. T.; Heineman, W. R. *J. Chem. Educ.* **1983**, *60*, 702−706. (d) Van Benschoten, J. J.; Lewis,

J. Y.; Heineman, W. R. *J. Chem. Educ.* **1983**, *60*, 772−776. (e) Mobbott, G. A. *J. Chem. Educ.* **1983**, *60*, 697−702.
(29) Lage, M. L.; Mancheño, M. J.; Martínez-Álvarez, R.; Gómez-Gallego, M.; Fernández, I.; Sierra, M. A. *Organometallics* **2009**, *28*, 2762−2772.
(30) See computational details.
(31) (a) Kemp, K. C.; Fourie, E.; Conradie, J.; Swarts, J. C. *Organometallics* **2008**, *27*, 353−362. (b) Conradie, J.; Swarts, J. C. *Dalton Trans.* **2011**, *40*, 5844−5851.
(32) Siegert, U.; Muller, T. J.; Swarts, J. C. *Polyhedron* **2013**, *51*, 41−45.
(33) (a) Conradie, J.; Swarts, J. C. *Eur. J. Inorg. Chem.* **2011**, 2439−2449. (b) Conradie, J.; Swarts, J. C. *Organometallics* **2009**, *28*, 1018−1026. (c) Connelly, N. G.; Geiger, W. E. *Chem. Rev.* **1996**, *96*, 877−910.
(34) This result is not surprising as the HOMO of the group 6 Fischer carbene complexes is located on the transition metal in most cases. See, for instance: (a) Fernández, I.; Sierra, M. A.; Cossío, F. P. *J. Org. Chem.* **2006**, *71*, 6178−6184. (b) Fernández, I.; Sierra, M. A.; Cossío, F. P. *J. Org. Chem.* **2008**, *73*, 2083−2089. (c) Andrada, D. M.; Granados, A. M.; Solà, M.; Fernández, I. *Organometallics* **2011**, *30*, 466−476.
(35) Bader, R. F. W. *Atoms in Molecules. A Quantum Theory*; Oxford University Press: Oxford, U.K., 1990.
(36) (a) Foster, J. P.; Weinhold, F. *J. Am. Chem. Soc.* **1980**, *102*, 7211−7218. (b) Reed, A. E.; Curtiss, L. A.; Weinhold, F. *Chem. Rev.* **1988**, *88*, 899−926.
(37) Lein, M. *Coord. Chem. Rev.* **2009**, *253*, 625−634.
(38) *APEX2* (including SAINT and SADABS); Bruker AXS Inc.: Madison, WI, 2013.
(39) Sheldrick, G. M.. *Acta Crystallogr.* **2008**, *A64*, 112−122.
(40) (a) Gritzner, G.; Kuta, J. *Pure Appl. Chem.* **1984**, *56*, 461−466. (b) Gagne, R. R.; Koval, C. A.; Lisensky, G. C. *Inorg. Chem.* **1980**, *19*, 2855−2857.
(41) Leading references describing the electrochemical activity and behavior of ferrocene and decamethylferrocene in a multitude of organic solvents are (a) Noviandri, I.; Brown, K. N.; Fleming, D. S.; Gulyas, P. T.; Lay, P. A.; Masters, A. F.; Phillips, L. *J. Phys. Chem. B* **1999**, *103*, 6713−6722. (b) Connelly, N. G.; Geiger, W. E. *Chem. Rev.* **1996**, *96*, 877−910. (c) Ruiz, J.; Astruc, D. *C.R. Acad. Sci. (Paris), Ser. IIc* **1998**, *1*, 21. (d) Aranzaes, R. J.; Daniel, M. C.; Astruc, D. *Can. J. Chem.* **2006**, *84*, 288−299. (e) Fourie, E.; Swarts, J. C.; Chambrier, I.; Cook, M. J. *Dalton Trans.* **2009**, 1145−1154.
(42) Frisch, M. J.; Trucks, G. W.; Schlegel, H. B.; Scuseria, G. E.; Robb, M. A.; Cheeseman, J. R.; Scalmani, G.; Barone, V.; Mennucci, B.; Petersson, G. A.; Nakatsuji, H.; Caricato, M.; Li, X.; Hratchian, H. P.; Izmaylov, A. F.; Bloino, J.; Zheng, G.; Sonnenberg, J. L.; Hada, M.; Ehara, M.; Toyota, K.; Fukuda, R.; Hasegawa, J.; Ishida, M.; Nakajima, T.; Honda, Y.; Kitao, O.; Nakai, H.; Vreven, T.; Montgomery, Jr., J. A.; Peralta, J. E.; Ogliaro, F.; Bearpark, M.; Heyd, J. J.; Brothers, E.; Kudin, K. N.; Staroverov, V. N.; Kobayashi, R.; Normand, J.; Raghavachari, K.; Rendell, A.; Burant, J. C.; Iyengar, S. S.; Tomasi, J.; Cossi, M.; Rega, N.; Millam, N. J.; Klene, M.; Knox, J. E.; Cross, J. B.; Bakken, V.; Adamo, C.; Jaramillo, J.; Gomperts, R.; Stratmann, R. E.; Yazyev, O.; Austin, A. J.; Cammi, R.; Pomelli, C.; Ochterski, J. W.; Martin, R. L.; Morokuma, K.; Zakrzewski, V. G.; Voth, G. A.; Salvador, P.; Dannenberg, J. J.; Dapprich, S.; Daniels, A. D.; Farkas, Ö.; Foresman, J. B.; Ortiz, J. V.; Cioslowski, J.; Fox, D. J. *Gaussian 09*, Revision B.1; Gaussian, Inc.: Wallingford, CT, 2009.
(43) (a) Becke, A. D. *J. Chem. Phys.* **1993**, *98*, 5648. (b) Lee, C.; Yang, W.; Parr, R. G. *Phys. Rev. B* **1988**, *37*, 785−789.
(44) Weigend, F.; Ahlrichs, R. *Phys. Chem. Chem. Phys.* **2005**, *7*, 3297−3305.
(45) Keith, T. A. *AIMAll*, 2010, http://tkgristmill.com